

Dynamics of Cryogenic Jets: Non-Rayleigh Breakup and Onset of Non-Axisymmetric Motions

A.V. Boukharov,¹ M. Büscher,^{2,*} A.S. Gerasimov,³ V.D. Chernetsky,³
P.V. Fedorets,^{2,3} I.N. Maryshev,¹ A.A. Semenov,¹ and A.F. Ginevskii¹

¹*Moscow Power Engineering Institute, Ul. Krasno-Kazarmennaja 13, 117218 Moscow, Russia*

²*Institut für Kernphysik, Forschungszentrum Jülich, 52425 Jülich, Germany*

³*Institute for Theoretical and Experimental Physics, B. Chermushkinskaya 25, 117218 Moscow, Russia*

(Dated: January 17, 2021)

We report development of generators for periodic, satellite-free fluxes of mono-disperse drops with diameters down to 10 μm from cryogenic liquids like H_2 , N_2 , Ar and Xe (and, as reference fluid, water). While the breakup of water jets can well be described by Rayleigh's linear theory, we find jet regimes for H_2 and N_2 which reveal deviations from this behavior. Thus, Rayleigh's theory is inappropriate for thin jets that exchange energy and/or mass with the surrounding medium. Moreover, at high evaporation rates, axial symmetry of the dynamics is lost. When the drops pass into vacuum, frozen pellets form due to surface evaporation. The narrow width of the pellet flux paves the way towards various industrial and scientific applications.

PACS numbers: 07.20.Mc, 07.90.+c, 29.25.Pj, 47.55.Dz, 52.50.Dg

Drop formation from incompressible liquids is ubiquitous in daily life and technology, and such processes have been at the focus of scientific investigations for almost two centuries [1, 2, 3, 4, 5, 6]. Even the simple case of jets emanating from a vibrating nozzle leads to a broad spectrum of drop sizes, and the existence of satellite drops [7]. However, for technologies like ink-jet printing [8], for laser-plasma UV sources [9], for compact laser-based particle accelerators [10], accelerator experiments [11], or for space operations [12], the drop sizes and rates must be highly homogeneous.

The disintegration of a slow cylindrical jet is caused by the growth of perturbations initiated at the ejection nozzle. An axially symmetric perturbation leads to jet breakup when its amplitude becomes equal to the jet radius. This domain is commonly denoted as the Rayleigh regime. In 1878 Lord Rayleigh described fluids in the limit of zero viscosity [2], while his 1892 paper [3] concerns the opposite limit where inertial effects are negligible compared to viscous ones. Rayleigh's work was extended by Chandrasekhar [4] to arbitrary viscosities. It has been shown [7] that the measurement of breakup lengths, *e.g.* for the forced breakup of water jets with precise control of the nozzle-perturbation frequency, allows for precise tests of linear theories, although the final stage of capillary pinching is non-linear [13].

Experimentally, the selection of a well defined initial surface-perturbation amplitude and a certain frequency is commonly achieved by using piezoelectric transducers. Most of the existing data have been obtained for water (or water-based ink) and fluids of higher viscosities, with jets emanating into air at normal pressure.

In this letter we report on first quantitative measurements of the breakup of cryogenic and water jets, injected into the same gaseous substance close to triple-point (TP) conditions (63 K and 125 mbar for N_2 , 14 K

and 70 mbar for H_2). In doing so we can widen the experimentally accessible parameter space, while keeping the Reynolds number $\text{Re}=(\rho \cdot v_{\text{jet}} \cdot R_0)/\mu$ (which represents the relative importance of inertial and viscous forces) and the Ohnesorge number $\text{Oh}=\mu/(\sigma \cdot \rho \cdot R_0)^{1/2}$ (viscous forces and surface tension) in the same range as for the existing water data. ρ (μ , σ) denote the fluid density (viscosity, surface tension), and v_{jet} (R_0) the jet velocity (initial jet radius). At TP pressures and jet velocities of a few m/s, aerodynamic interactions with the ambient medium are small and, thus, we are close to the ideal case of an inviscid jet breaking up in vacuum and our data allow for clean tests of Rayleigh's theory.

According to the linear theory, a small surface perturbation δ (measured in units of R_0) of a jet moving into z -direction, imposed at the nozzle exit ($z=0$) with frequency f , grows exponentially towards the jet axis [2, 14]. Then, the minimum (over time) necking of the jet $R(z)$ at a certain distance z from the nozzle is

$$\frac{R(z)}{R_0} = 1 - \delta \exp\left(\frac{\gamma/\gamma_0}{\text{Oh} \cdot \text{Re}} \cdot \frac{z}{R_0}\right). \quad (1)$$

The dimensionless growth rate γ/γ_0 depends on the wavelength λ of the perturbation and can be expressed in terms of a reduced wave number $X=2\pi \cdot R_0/\lambda = 2\pi \cdot R_0 \cdot f/v_{\text{jet}}$ for $X < 1$ and $\text{Re} \cdot \text{Oh} \gg 1$:

$$\frac{\gamma}{\gamma_0} = -\frac{3}{2}\text{Oh}X^2 + \sqrt{\frac{9}{4}\text{Oh}^2X^4 + \frac{1}{2}X^2(1-X^2)} \quad (2)$$

with $\gamma_0=\text{Oh} \cdot (\sigma/\mu R_0)$. Figure 1 shows a plot of Eq.(2) for water, N_2 and H_2 jets; linear theory predicts a practically identical X dependence of γ/γ_0 for all three liquids. If $\text{Re} \cdot \text{Oh}$ approaches unity, the theory tends to underestimate γ/γ_0 , see *e.g.* the discussion by Kalaaaji et al. [7].

Since a jet breaks into drops for $R(z)=0$, the jet length

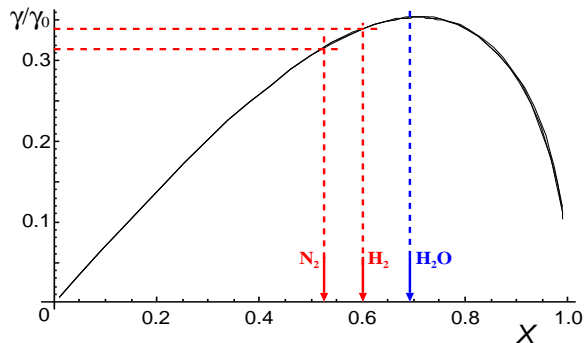


FIG. 1: Dimensionless growth rate γ/γ_0 as a function of the reduced wave number X in linear theory. For N_2 and H_2 two (practically identical) curves have been calculated with Eq.(2) using the Oh values from Table I. For water a typical Ohnesorge number $Oh=0.02$ has been chosen, since γ/γ_0 behaves similarly at $Oh < 0.1$. The arrows indicate the X -values for which we have observed satellite-free drop production.

L_{jet} results from Eq.(1) as:

$$L_{jet} = \frac{R_0}{\gamma/\gamma_0} \text{Re} \cdot \text{Oh} \ln(1/\delta) = \frac{v_{jet}}{\gamma/\gamma_0} \sqrt{\frac{\rho R_0^3}{\sigma}} \ln(1/\delta) \quad (3)$$

Relations (1)–(3) have been experimentally verified in numerous studies with water or viscous fluids [7, 15]. Satellite-free and mono-disperse water-drop production has also been reported: for not too large values of δ ($\lesssim 0.01$) it only occurs at maximum values of γ/γ_0 , *i.e.* at $X_{max}=0.69$ [16, 17].

Quantitative studies of forced jet break-up depend crucially on the suppression of unwanted nozzle vibrations which can, *e.g.*, be caused by cold head units [18]. Thus our drop generator [19] is surrounded by a cryostat with baths of liquid N_2 and He, see Fig. 2. Liquefaction of H_2 is achieved in three stages: first cooling with liquid N_2 , further cooling in a heat exchanger by evaporated He, and final cooling in the condenser by cold He gas. For production of, *e.g.*, N_2 and Ar jets, cooling with liquid N_2 is sufficient while for water we use a dedicated generator without cooling cryostat. The temperatures along the main gas and liquid flows are controlled with an accuracy of 0.1 K. From the condenser, the liquid passes through the vibrating nozzle and reaches the triple-point chamber (TPC) where the jet disintegrates into drops. The liquid temperature in the nozzle is maintained slightly below the boiling point and, according to simulation calculations, the temperature decrease in the jet until break-up from heat exchange in the TPC is below 0.2 K (cf. Table I). Therefore, the generation of semi-solid domains can be excluded. The temperatures and pressures in the TPC are kept over several hours within ± 0.2 K (± 0.2 mbar) at the nominal values.

Two nozzle types have been utilized, glass nozzles in brass housings and such made from stainless steel. The former, with inner diameters of 12–30 μm at the nozzle

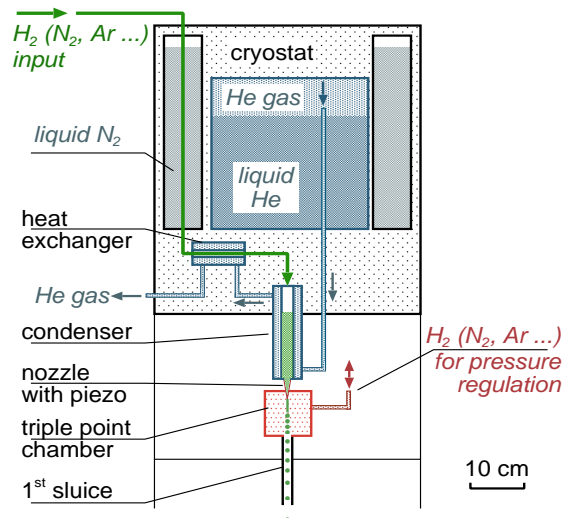


FIG. 2: (Color online) Sketch of the drop generator. The cryostat (total height ~ 0.8 m, not drawn to scale) comprises the cooling liquids (N_2 and He) as well as the heat exchanger and the upper part of the condenser. These are cooled by a stream of evaporated He gas. The condenser houses a few cm^3 of the cryogenic liquid which is driven through a nozzle into the TPC by overpressure. Constant pressure in the TPC is maintained by an auxiliary gas feeding.

tip, have the advantage of a smooth internal surface and allow one to look inside the channel during operation. The 16–30 μm steel nozzles offer high shape reproducibility and smaller length-to-diameter ratios of the holes, allowing operation with lower jet-driving pressures. The results presented here have been obtained with glass nozzles and pressures of ~ 0.4 – 0.9 bar for H_2 and ~ 1.0 – 1.5 bar for N_2 . Higher pressures lead to higher jet veloc-

TABLE I: Parameters of the jets from Fig. 3. γ/γ_0 is calculated with Eq.(2), the jet length $L_{jet}^{\text{Rayleigh}}$ with Eq.(3).

| | N_2 | H_2 |
|---|-----------|-----------|
| Density ρ (kg/m^3) [20, 21] | 823.7 | 64.04 |
| Static surface tension σ (N/m) [20, 21] | 0.0094 | 0.0025 |
| Viscosity μ ($\text{mPa} \cdot \text{s}$) [20, 21] | 0.2113 | 0.0183 |
| TPC pressure (mbar) | 300 | 130 |
| TPC temperature (K) | 74 | 17 |
| Jet temperature (K) | 77.2–77.0 | 20.0–19.8 |
| Nozzle frequency f (kHz) | 26 | 38 |
| Jet diameter $2R_0$ (μm) | 17 | 12 |
| Jet velocity v_{jet} (m/s) | 2.6 | 2.4 |
| Reduced wave number X | 0.53 | 0.60 |
| Reynolds number Re | 84 | 50 |
| Ohnesorge number Oh | 0.026 | 0.019 |
| $\text{Re} \cdot Oh$ | 2.2 | 1.0 |
| Growth rate γ/γ_0 | 0.31 | 0.34 |
| Initial perturbation δ | 0.02 | 0.02 |
| Expected jet length $L_{jet}^{\text{Rayleigh}}$ (μm) | 240 | 70 |
| Measured jet length L_{jet} (μm) | 310 | 290 |

ities. The piezo-electric transducer allows us to excite sinusoidal nozzle vibrations in the range $f=1\text{--}60\text{ kHz}$.

The jet decay has been observed with two perpendicularly placed CCD cameras and strobe lamps that are triggered synchronously to the nozzle, with a 10 times lower frequency, and a flash duration of $\sim 1.5\ \mu\text{s}$. The jet diameter $2R_0$ has been assumed to be equal to the nozzle diameter which is correct to better than $\pm 10\%$ [7]. This is confirmed by our measurement of jet diameters with the CCD cameras. v_{jet} has been determined by measuring the wave-propagation velocity along the jet surface. The initial amplitude δ has been derived from reference measurements of water jet lengths using Eq.(3), as well as from direct amplitude measurements with an Michelson interferometer. See Ref. [15] for further details of the jet diagnostics.

Figure 3 shows the breakup of N_2 and H_2 jets; for certain choices of the jet and TPC parameters (see Table I), satellite-free and mono-disperse drop production is achieved. Astonishingly, we find it at $X=0.53$ and $X=0.60$, respectively, *i.e.* for different wave numbers as compared to water. Since this is off the maximum from Fig. 1, it suggests an X dependence of γ/γ_0 different from Eq.(2). In order to further test a possible deviation from Rayleigh-like behavior, we have checked the validity of Eqs. (1)–(3) in more detail.

The last two lines of Table I compare the measured and predicted jet-decay lengths; it is seen that the cryogenic jets are much longer than expected. This cannot be explained by a variation of the parameters that enter Eq.(3). For example, an unphysical value of $\delta=10^{-8}$ would be required to yield the large decay length of the H_2 jet. The dynamic surface tension can differ from the static values for σ quoted in Table I, it had to be, however, 20 (2) times smaller to explain the observed H_2 (N_2) jet lengths which seems unreasonable.

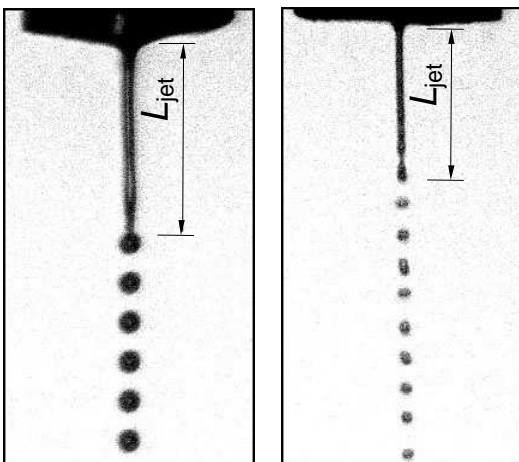


FIG. 3: First observation of satellite-free and monodisperse disintegration of N_2 (left) and H_2 (right) jets. In the upper edge of the photos the tip of the vibrating nozzle can be seen.

An explanation of the obvious violation of Rayleigh's theory might be disturbances like temperature, pressure and surface-tension variations as well as liquid-gas transitions. It has, *e.g.*, been predicted [22] that evaporation and condensation decrease L_{jet} (which seems to contradict the large measured L_{jet} values from Table I) and, for large evaporation rates, satellite production can be suppressed. One may presume that for our jets evaporation is strong since in the TPC jets and ambient gas coexist close to the vapor-pressure curve. In order to test the effect of evaporation we have enhanced it by reducing the jet velocities or the TPC pressure (keeping the other parameters constant). This leads to a phenomenon, to our knowledge not reported until now. The jets slowly move from their vertical flux direction to one off the nozzle symmetry axis while preserving their smooth surfaces. The direction they choose seems to be random. However, once a jet has arrived at a certain stable configuration it may stay there for seconds; only at very small jet-bending radii are frequent abrupt changes of the jet directions observed. As an example we show in Fig. 4 N_2 , H_2 and water jets. Even back-bending is observed in some cases. Systematic studies reveal larger jet deflections from the vertical axis with decreasing jet diameter and velocity or TPC pressure. We note that asymmetric heating has been employed by another group to deflect liquid micro-jets [23], however, we report spontaneous deflection of symmetrically produced jets.

When the drops leave the TPC through a 1st sluice into a subsequent chamber ($p=o(10^{-2})$ mbar), they freeze to pellets due to strong surface evaporation, and are accelerated by the gas flow from the TPC. Then the pellets pass a 2nd sluice and a 2nd chamber ($o(10^{-4})$ mbar), and finally reach a dummy scattering chamber through a thin tube ($\varnothing \sim 2$ cm), which is located 1.2 m downstream of the TPC. In order to minimize turbulences of the gas flow in the 1st sluice (and, thus, distortions of the produced pellets) it has a circular cross section with a radius that decreases exponentially to $600\ \mu\text{m}$ in flight direction. For pellet observation two CCD cameras have been positioned at the outlet of the 1st sluice or at the dummy chamber. Stable H_2 and N_2 pellet production with diam-

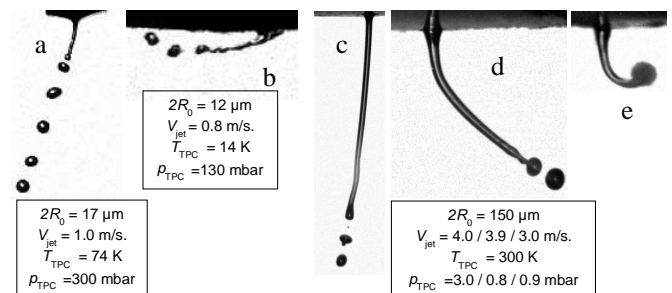


FIG. 4: First observation of non-axisymmetric N_2 (a), H_2 (b) and water (c–e) jets.

eters 20–40 μm (the pellet diameter is about two nozzle diameters) has been observed. Deviations from the mean pellet diameter are below 1% (10%) over periods of few seconds (hours). The average velocity of 30 μm pellets amounts to ~ 70 m/s. The radial displacement of the pellets from their nominal flight path in the dummy chamber of about ± 200 μm has been extrapolated from the angular pellet distributions measured behind the 1st sluice. This value is dominated by our experimental resolution. The small pellet-beam divergence is a consequence of the extremely regular jet breakup in the TPC (Fig. 3).

If used as an internal target at a storage ring, our device minimizes unwanted gas loads to the accelerator and allows for an effective target thickness of a few 10^{15} atoms/cm². Since the tube connecting the generator with the interaction zone is rather narrow, detectors can be placed close to the interaction point in a nearly 4π configuration. Such a geometry is also advantageous for placing collector mirrors in laser-plasma UV sources [9]. In addition, the large separation of the hot and radiating plasma from the jet generator makes such a set-up especially favorable.

In this letter we present first data on the mono-disperse breakup of cryogenic jets. We find that the jets are significantly more resistant to breakup than predicted by Rayleigh's theory. We suggest that a reason for this discrepancy is the influence of evaporation effects. This interpretation is supported by the observation of non-axially symmetric jets. This new jet mode — for which so far not even a rudimentary theoretical explanation has been formulated — sets in when one decreases the ambient pressure very close to the triple-point values. For a complete theoretical delineation of drop formation processes from thin cryogenic jets, further systematic data, like on the X dependence of γ/γ_0 and the pressure dependence of L_{jet} , are required.

This work has been supported by BMBF (WTZ), COSY-FFE, DFG, EU (FP6), INTAS, ISTC, RFFI (07-08-00747a, 08-08-91950-NNIO_a), RMS, and the PANDA collaboration. The Russian team members thank for the hospitality at the FZJ, in particular for the support by H.Ströher. We acknowledge discussions with H.Calen, C.Ekström and Ö.Nordhage.

* E-mail: m.buescher@fz-juelich.de

- [1] F. Savart, *Ann. de Chim.* **53**, 337 (1833).
- [2] Lord Rayleigh, *Proc. London Math. Soc.* **s1-10**, 4 (1878).
- [3] Lord Rayleigh, *Philos. Mag.* **34**, 145 (1892).
- [4] S. Chandrasekhar, The capillary instability of a liquid jet. *In Hydrodynamic and Hydromagnetic Stability*, p. 537. Oxford Univ. Press (1961).
- [5] J. Eggers, *Rev. of Mod. Phys.* **69**, 865 (1997).
- [6] S.P. Lin and R.D. Reitz, *Annu. Rev. Fluid Mech.* **30**, 85 (1998).
- [7] A. Kalaaji, B. Lopez, P. Attane, and A. Soucemarianadin, *Phys. Fluids* **15**, 2469 (2003).
- [8] O.A. Basaran, *AICHE J.* **48**, 1842 (2002).
- [9] B.A.M. Hansson and H.M. Hertz, *J. Phys. D* **37**, 3233 (2004).
- [10] S. Ter-Avetisyan, M. Schnürer, P.V. Nickles, M. Kalashnikov, E. Risse, T. Sokollik, W. Sandner, A. Andreev, and V. Tikhonchuk, *Phys. Rev. Lett.* **96**, 145006 (2006).
- [11] Ö. Nordhage, Z.-K. Li, C.-J. Friden, G. Norman, U. Wiedner, *Nucl. Instrum. Meth. A* **546**, 391 (2005).
- [12] E.P. Muntz and M. Dixon, *J. Spacecraft Rockets* **23**, 411 (1986).
- [13] N. Ashgriz, and F. Mashayek, *J. Fluid. Mech.* **291**, 163 (1995); R. Suryo, P. Doshi, and O.A. Basaran, *Phys. Fluids* **18**, 082107 (2006).
- [14] V.V. Blazhenkov, A.F. Ginevskii, V.F. Gunbin, A.S. Dmitriev, and S.I. Tscheglov, *Fluid Dynamics* **30**, 544 (1995).
- [15] V.V. Blazhenkov, A.F. Ginevskii, V.F. Gunbin, A.S. Dmitriev, and A.I. Motin, *J. Eng. Phys. Thermophys.* **55**, 994 (1988).
- [16] V.V. Blazhenkov, A.F. Ginevskii, V.F. Gunbin, and A.S. Dmitriev, *Fluid Dynamics* **23**, 203 (1988); V.V. Blazhenkov, A.F. Ginevskii, V.F. Gunbin, A.S. Dmitriev, and A.I. Shcheglov, *Fluid Dynamics* **28**, 338 (1993).
- [17] W.T. Pimbley, and H.C. Lee, *IBM J. Res. Dev.* **21**, 21 (1977).
- [18] Ö. Nordhage, Ph.D. Thesis, Acta Universitatis Upsalensis (2006); <http://publications.uu.se/abstract.xsql?dbid=7137>
- [19] Russian Federation Patent No. 2298890; German Patent Application No. 10 2007 017 212.7-13
- [20] D.U. Hamburg and N.F. Dubrovkin, Hydrogen: properties, generation, storage, transport, application, Chemistry Publishing, Moscow (1989), ISBN 5-7245-0034-5, pp. 109, 142, 174 (in Russian).
- [21] M.P. Malkov (ed.), Handbook of physical and technical fundamentals of cryogenics, Energoatomizdat Publishing, Moscow (1963) pp. 90, 123, 176 (in Russian).
- [22] M. Saroka, Y. Guo, and N. Ashgriz, *AIAA J.* **39**, 1728 (2001); S. Savtchenko, and N. Ashgriz, *Phys. Fluids* **17**, 112102 (2005).
- [23] J.M. Chwalek *et al.*, *Phys. Fluids* **14**, L37 (2002).